LA-UR -86-2271

CONF-8606165--2

Received by OSTI

AUG 0 5 1986

LA-UR--86-2271

DE86 013861

TITLE:
COMPARISONS OF THE STRUCTURE, STABILITY, AND ELECTRON DISTRIBUTION OF NITROBENZENES AND NITRO-SYM-TRIAZINES

AUTHOR(S): James P. Ritchie, T-14

SUBMITTED TO: Gordon Research Conferences
"Electron Distributions and Chemical Bonding"
Plymouth, New Hampshire
June 30 - July 4, 1986

Los Alamos
Los Alamos National Laboratory
Los Alamos, New Mexico 87545

Comparisons of the Structure, Stability, and Electron Distribution of Nitrobenzenes and Nitro-sym-triazines

by

James P. Ritchie
MS-B214
Los Alamos National Laboratory
Los Alamos, NM 87545

Nitrobenzenes are a well known class of stable organic compounds. Nitro-sym-triazines are not known, although other substituted triazines are very well known. To investigate the what properties the nitrotriazines might have, should they be synthesized, we performed molecular orbital calculations for nitrotriazine (NTZ), dinitrotriazine (DNTZ), and trinitrotriazine (TNTZ). Nitrobenzenes with analogous nitro group substitution were also studied to provide a check on the calculations. In particular, nitrobenzene (NB), 1,3-dinitrobenzene (DNB), and 1,3,5-trinitrobenzene (TNB) were studied.

Methods

Molecular orbital calculations employing the 3-21G basis set were performed with the Gaussian 82 program. Geometrical parameters were optimized within the stated point group to obtain final energies. Further calculations were also performed to determine if twisting the nitro groups out of the plane resulted in higher energies. For the nitrobenzenes studied, non-planar geometries were higher in energy than planar ones. For the nitrotriazines, a non-planar geometry was higher in energy for nitrotriazine, but dinitrotriazine and trinitrotriazine prefer non-planar structures. Deviations from planarity have little effect upon the calculated energies of either the nitrobenzenes or nitrotriazines; therefore, it would not be too surprising if these compounds turn out to be non-planar in crystals, due to packing forces. Additionally, our calculations, which are based upon planar models, are adequate for the purpose at hand.

Thermodynamic calculations to obtain heats of formation at 25 C were performed by deriving energy increments for the C_{ar}-H, N_{ar}, and C_{ar}-NO_2 groups. The energy increment for the C-H group was obtained as 1/6 the calculated total energy of benzene plus its heat of formation at 25 C. Next, knowing the Car-H increment, the N_{ar} and C-NO_2 increments were obtained from the calculated total energies of pyridine and nitrobenzene, respectively. These compounds were chosen because reliable thermodynamic data is available for them. As a result, our calculations exactly reproduce the observed data for the reference compounds. The final energy increments obtained are shown in Table I.

Electron distributions and atom-centered multipole expansions were calculated using the programs RHO and RHODER. These programs assign charge to atoms in a molecule according to Hirshfeld's Stockholder recipe. This method depends on the construction of a promolecule, which is the superposition of spherically averaged atom densities. Charge is assigned in the same proportion to the atom in the molecule as it donates charge to the promolecule.

Additionally, density deformation maps are formed by subtracting the promolecule's electron density from that of the molecule.

Results

Table II shows the calculated heats of formation of the nitrobenzenes and nitrotriazines. Calculated total energies, HOMO and LUMO energies, and dipole moments are shown in Table III. It should be noted that the experimental dipole moment of nitrobenzene has been determined to be 4.0 D, suggesting that the calculations overestimate the electron withdrawing ability of the nitro group.

Thermodynamics: The calculated heats of formation of the nitrobenzenes and nitrotriazines show very different behavior. While the heats for formation of the benzenes change only slightly with increasing nitro group substitution, the triazines show a large increase in the heat of formation with the substitution of each nitro group. Indeed the first nitro group in benzene lowers the heat of formation from that in benzene, while subsequent substitution raises the heat of formation by 1 and 5 kcal. Substitution of nitro groups raises the heat of formation of triazine by 11.1, 16.7, and 21.6 kcal. These results show that substitution of a nitro group in triazine is thermodynamically destabilizing relative to the substitution of a nitro group in benzene.

Structure: The calculated structures for the nitrobenzenes and nitrotriazines are shown in Figures 1-6, while calculated structures for benzene, pyridine and triazine are shown in Figures 7, 8 and 9.

Comparing the nitro groups in the compounds, it is found that the nitro group geometry remains nearly constant in the triazine series and in the benzene series. Comparing triazines and benzenes, it is consistently found that the C-N bond is longer and the N-O bonds shorter in the triazines than in the benzenes. These results are consistent with the greater contribution in the benzenes of charge-bearing nitro group resonance structures.

The ring geometries can not be understood in terms of the contribution of charge-bearing nitro group resonance structures. Such structures place positive charges on the ortho and para positions and double bonds between the meta and either the para or ortho position, as illustrated below. Rather, these structures seem better explained by the sigma withdrawing ability or inductive effect of the nitro group. This results, in nitrobenzene for example, in bond lengths that are shortest nearest the nitro groups and that become longer with increasing distance from the nitro group.

Likewise, in nitrotriazine the shortest ring bond is nearest the nitro group, while the remaining bonds are longer. Here the effect is not apparent beyond the adjacent bond.

Electron Distributions: Calculated Hirshfeld charges are shown in Table Iv for the nitrobenzenes and in Table V for the nitrotriazines. In general, these charges illustrate that the nitro group is strongly electron withdrawing. Increasing nitro group substitution, while withdrawing greater amounts of charge from the ring, results in lesser electron populations in each individual nitro group. The ipso position is always most electron deficient, showing that sigma withdrawal dominates at this position over pi resonance effects, which would place a negative charge on the ipso carbon.

Charges at the para position are consistent with the operation of pi withdrawing effects. Thus, of the three ring positions, the para position is most electron poor, the ortho is less so, while the meta position is least electron deficient. It is somewhat unusual that the ortho position should be less electron deficient that the para position, because both sigma and pi withdrawing effects are expected to be stronger at the ortho position.

Figure 10-13 show density deformation maps and electrostatic potentials calculated for the nitrotriazines and Figures 14-17 show similar results for nitrobenzenes. The density deformation maps show precisely what changes in electron density occur to produce the indicated electrostatic potential. Thus, the atom-centered multipole expansions describe how the molecule differs from a superposition of spherical neutral atoms; ie, the promolecule. Because the electrostatic potential is zero outside a spherical neutral charge distribution, if it is assumed that van der Waals spheres enclose all the electron density of the promolecule, then it follows that the electrostatic potential of the promolecule is zero at distances greater than a van der Waals radius. (Actually, van der Waals spheres are found to enclose only about 99.5% of the promolecule's electronic charge.)

The electrostatic potentials show that increasing nitro group has the effect of making the electrostatic associated with the pi system much more positive. In the triazine series, the electrostatic potential goes from a maximum value of about 35 kcal in triazine to greater than 70 kcal in trinitrotriazine. A similar trend is found in the benzenes, where a negative potential associated with the pi system in benzene is changed to a +40 kcal potential in trinitrobenzene.

Discussion

The nitrotriazines and nitrobenzenes are found to differ in several important respects. The thermodynamic effect of nitro group substitution differs significantly, destabilizing the triazine relative to the benzene. The calculated structures suggest that the pi withdrawing effect of the nitro group is not the dominant factor in determining geometries. The sigma withdrawing ability of the nitro group is quite strong and provides a better rationalizaiton of the calculated geometries. Nevertheless, the pi withdrawing effect is found to rationalize some of the calculated charges. Taken together the sigma and pi withdrawing nature of the nitro group results in large changes in the electrostatic potentials of the triazines. The large positive changes in the potentials associated with the pi system suggest that nitro group substitution makes the pi system more reactive toward nucleophiles. Indeed, Miesenheimer complexes of nitro benzenes are well known. The greater magnitude of the potentials associated with the pi system of the triazines suggests that the triazines would likely be more reactive toward nucleophiles than nitrobenzenes.

A final consideration involves the stability of the nitrotriazines. It has been proposed that nitro aromatics and heteroaromatics can undergo decomposition via the nitro-nitrite rearrangement. The results of our calculations show the triazine N to be a stronger electron withdrawer than a C-H fragment. Thus the nitro-nitrite rearrangement would be expected to proceed more quickly for the nitrotriazines than for the nitrobenzenes. Contributions from resonance structures such as that below would help stabilize the transition state.

Conclusions

Nitrotriazines are thermodynamically destabilized by nitro groups. Compared with nitrobenzenes the nitrotriazines are expected to be less stable thermodynamically, more susceptible to the nitro-nitrite rearrangement, and more reactive toward nucleophiles.

Table IV. Calculated Hirshfeld charges for nitrobenzenes.

Position	Benzene	NB	DNB	TNB
C_1	-.0491	.0112	.0177	.0241
C_2	-.0491	-.0290	-.0136	.0090
C_3	-.0491	-.0395	.0177	.0241
C_4	-.0491	-.0186	-.0028	.0090
C_5	-.0491	-.0395	-.0298	.0241
C_6	-.0491	-.0290	-.0028	.0090
H_1	.0491			
H_2	.0491	.0648	.0768	.0849
H_3	.0491	.0594		
H_4	.0491	.0615	.0746	.0849
H_5	.0491	.0594	.0689	
H_6	.0491	.0648	.0746	.0849
N		.3000	.3013	.3024
O		-.2328	-.2240	-.2103
O'		-.2328	-.2180	-.2103

Table V. Calculated Hirshfeld charges for nitrotriazines.

Position	s-Triazine	NTZ	DNTZ	TNTZ
N_1	-.2016	-.1747	-.1530	-.1340
C_2	.1247	.1840	.1988	.2129
N_3	-.2016	-.1747	-.1532	-.1340
C_4	.1247	.1466	.1988	.2129
N_5	-.2016	-.1770	-.1530	-.1340
C_6	.1247	.1466	.1673	.2129
H_2	.0770			
H_4	.0770	.0909		
H_6	.0770	.0909	.1034	
N		.2888	.2907	.2924
O		-.2107	-.2016	-.1856
O'		-.2107	-.1935	-.1856

Table I. Derived energy increments obtained with the 3-21G basis set. These increments are derived from the known heats of formation and calculated energies of benzene, pyridine, and nitrobenzene. See text for details. 1 a.u.=627.51 kcal.

Group	Energy Increment (au)
C_{ar}-H	- 38.241 836
N_{ar}	- 54.157 886
C_{ar}-NO_2	-240.528 735

Table II. Estimated heats of formation in the gas phase at 25° in kcal/mol calculated using the energy increments in Table I and the results of molecular orbital calculations. Values for benzene, pyridine, and nitrobenzene were used to determine the energy increments and thus are reproduced exactly. Otherwise, the estimated accuracy is about ± 5 kcal.

Compound	$H_f^{298}(g)$	Obs.
Benzene	19.8	19.8[a]
Nitrobenzene	16.2	16.2[b,c]
1,3-Dinitrobenzene	17.2	12.8±.5[d]
1,3,5-Trinitrobenzene	22.2	14.9
Pyridine	34.6	34.6[a]
Sym-triazine	61.5	
Nitro-*s*-triazine	72.6	
1,3-Dinitro-*s*-triazine	89.3	
1,3,5-Trinitro-*s*-triazine	110.9	

[a] "Thermochemistry of Organic and Organometallic Compounts," by J. D. Cox and G. Pilcher; Academic Press: New York; 1970.

[b] K. Kusano, I. Wadso <u>Bull. Chem. Soc. Japan</u> 4, 1705 (1971).

[c] N. D. Lebedeva, Y. A. Katin, B. Y. Akhmedova <u>Russ. J. Phys. Chem.</u> **45**, 1192 (1971).

[d] N. D. Lebedeva, V. L. Ryadnenko, I. N. Kuznetsova <u>Russ. J. Phys. Chem.</u> **45**, 549 (1971).

Table III. Calculated total energies (in au), Highest Occupied Molecular Orbital (HOMO) and Lowest Unoccupied Molecular Orbital (LUMO) energies (in eV), and dipole moments (in Debye). According to Koopman's theorem, the HOMO and LUMO energies are equal to the negative of the ionization potential and electron affinity, respectively.

Molecule	Total Energy	E(HOMO)	E(LUMO)	Dipole
Benzene	-229.41945	- 9.2	4.1	0.0
Nitrobenzene	-479.37032	-10.2	1.2	5.3
Dinitrobenzene	-633.99746	-11.3	0.3	5.0
Trinitrobenzene	-836.27626	-12.3	-0.4	0.0
s-triazine	-277.10111	-11.6	2.7	0.0
Nitrotriazine	-479.37032	-11.8	0.3	4.7
Dinitrotriazine	-681.63062	-12.4	-0.8	4.5
Trinitrotriazine	-883.88307	-12.9	-1.6	0.0

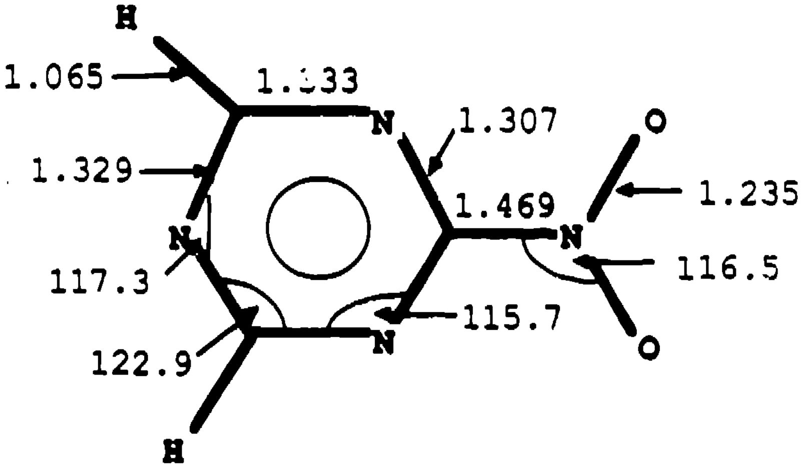

Figure 1. Calculated structure of nitro-*s*-triazine. Bond lengths in Å, angles in degrees. Symmetry group C_{2v}.

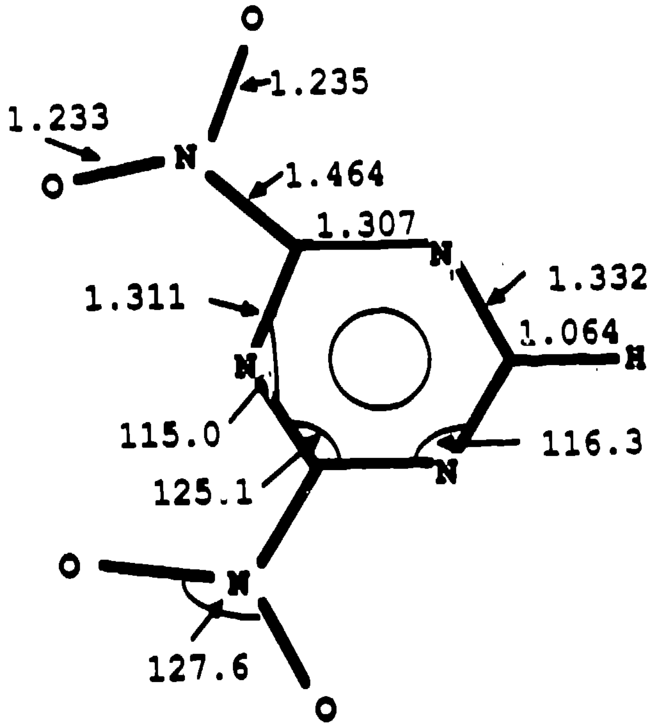

Figure 2. Calculated structure of 1,3-dinitro-*s*-triazine. Symmetry group C_{2v}.

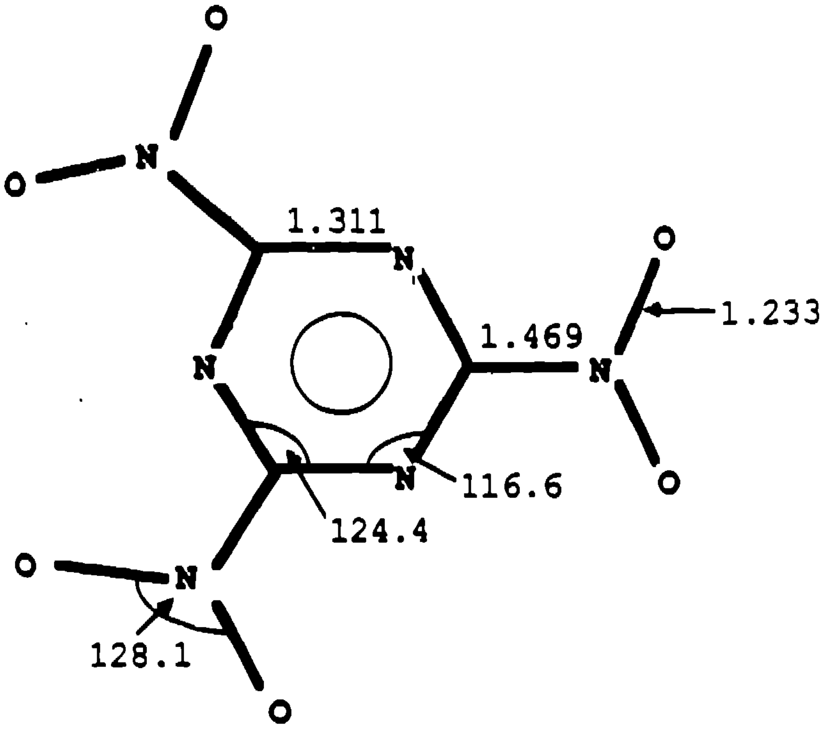

Figure 3. Calculated structure of 1,3,5-trinitro-*s*-triazine. Symmetry group D_{3h}.

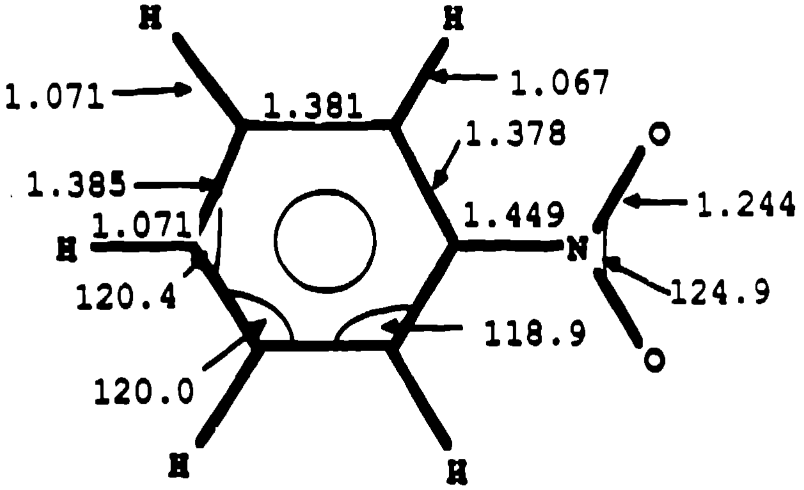

Figure 4. Calculated structure of nitrobenzene. Symmetry group C_{2v}. See J. Trotter *Tetrahedron*, 8, 13 (1960) for an X-ray investigation.

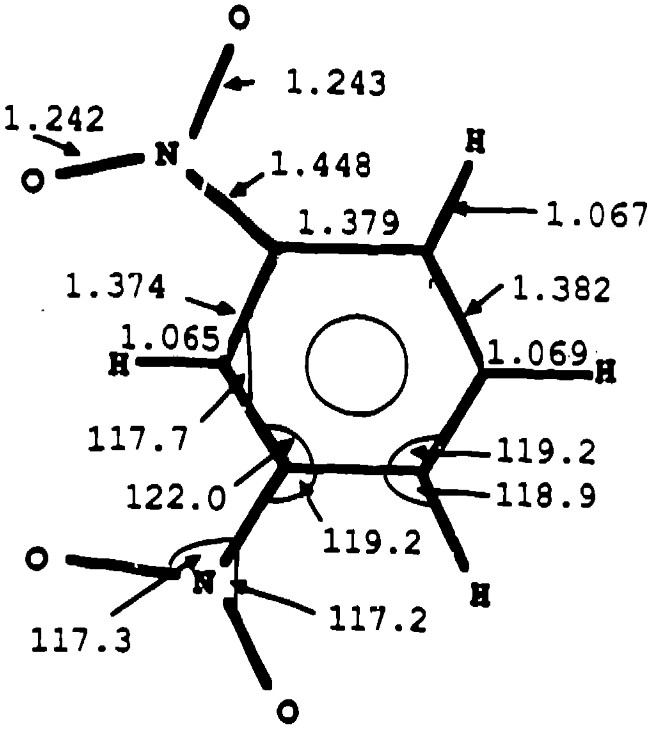

Figure 5. Calculated structure of 1,3-dinitrobenzene. Symmetry group C_{2v}. J. Trotter and C. S. Williston, <u>Acta Cryst.</u>, <u>21</u>, 285 (1966) for an X-ray investigation.

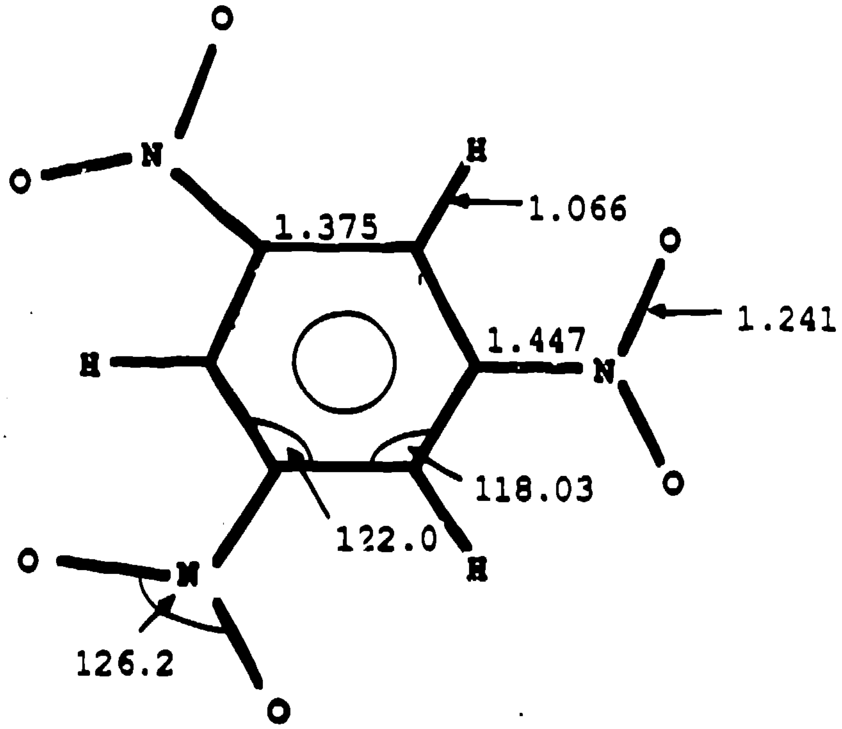

Figure 6. Calculated structure of 1,3,5-trinitrobenzene. Symmetry group D_{3h}. See C. S. Choi and J. E. Abel, <u>Acta Cryst.</u> <u>B28</u>, 193 (1972) for a neutron powder investigation.

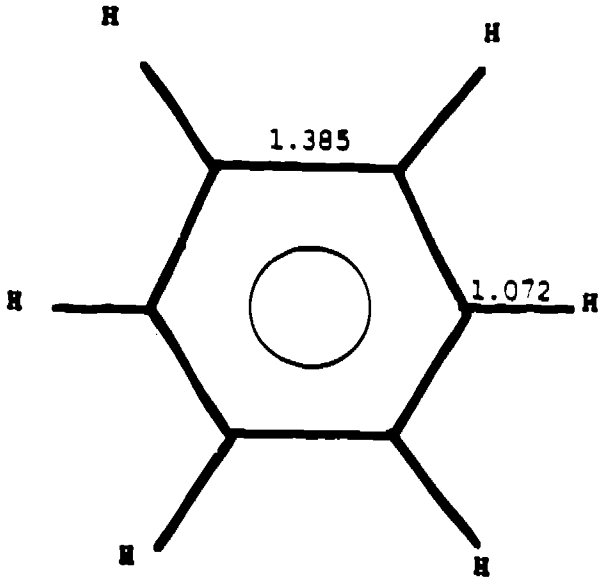

Figure 7. Calculated structure of benzene. Symmetry group D_{6h}. Experimentally, the C-C bond is 1.392 Å.

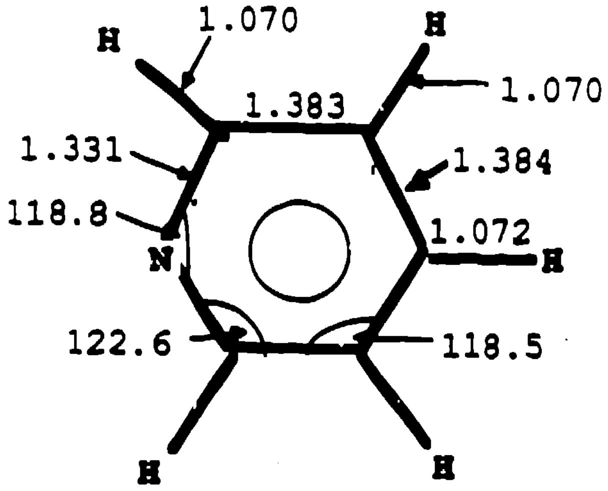

Figure 8. Calculated structure of pyridine. Symmetry group C_{2v}. See B. Bak, L. Hansen-Nygaard, and J. Rastrup-Andersen, *J. Mol. Spectrosc.* **2**, 361 (1958) for an experimental structure.

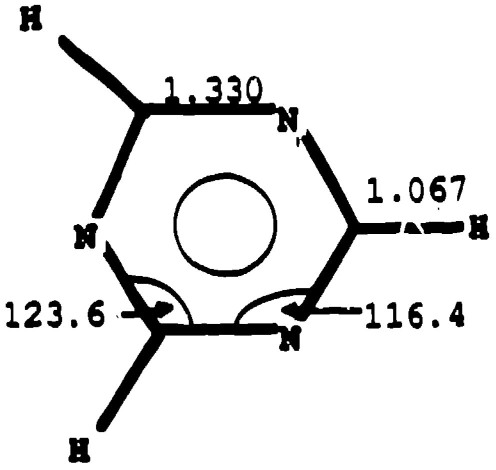

Figure 9. Calculated structure of *s*-triazine. Symmetry group D_{3h}.

Figure Captions

Figure 10. Density deformation maps (left) and electrostatic potentials (right) for sym-triazine in the molecular plane (upper) and in the perpendicular symmetry plane (lower). Atoms in the illustrated plane are indicated with a dark circle. Atoms projected into the illustrated plane are indicated with a +. Positive values are represented by the solid contours, negative values are represented by dashed countours, and zero as a values is represented by the combination dot-dot-dash contour. Regions within .2 A of the atoms in the DDM's is blanked to highlight the atom positions. Regions within a van der Waals radius of an atom are blanked in the electrostatic potential maps because the atom-centered multipole expansions are invalid there.

Figure 11. Density deformation maps (left) and elextrostatic potentials (right) for nitrotriazine in the molecular plane (upper) and in the perpendicular symmetry plane (lower). See Figure 10 for details.

Figure 12. Density deformation maps (left) and elextrostatic potentials (right) for dinitrotriazine in the molecular plane (upper) and in the perpendicular symmetry plane (lower). See Figure 10 for details.

Figure 13. Density deformation maps (left) and elextrostatic potentials (right) for trinitrotriazine in the molecular plane (upper) and in the perpendicular symmetry plane (lower). See Figure 10 for details.

Figure 14. Density deformation maps (left) and elextrostatic potentials (right) for benzene in the molecular plane (upper) and in the perpendicular symmetry plane (lower). See Figure 10 for details.

Figure 15. Density deformation maps (left) and elextrostatic potentials (right) for nitrobenzene in the molecular plane (upper) and in the perpendicular symmetry plane (lower). See Figure 10 for details.

Figure 16. Density deformation maps (left) and elextrostatic potentials (right) for 1,3-dinitrobenzene in the molecular plane (upper) and in the perpendicular symmetry plane (lower). See Figure 10 for details.

Figure 17 Density deformation maps (left) and elextrostatic potentials (right) for 1,3,5-trinitrobenzene in the molecular plane (upper) and in the perpendicular symmetry plane (lower). See Figure 10 for details.

Figure 10

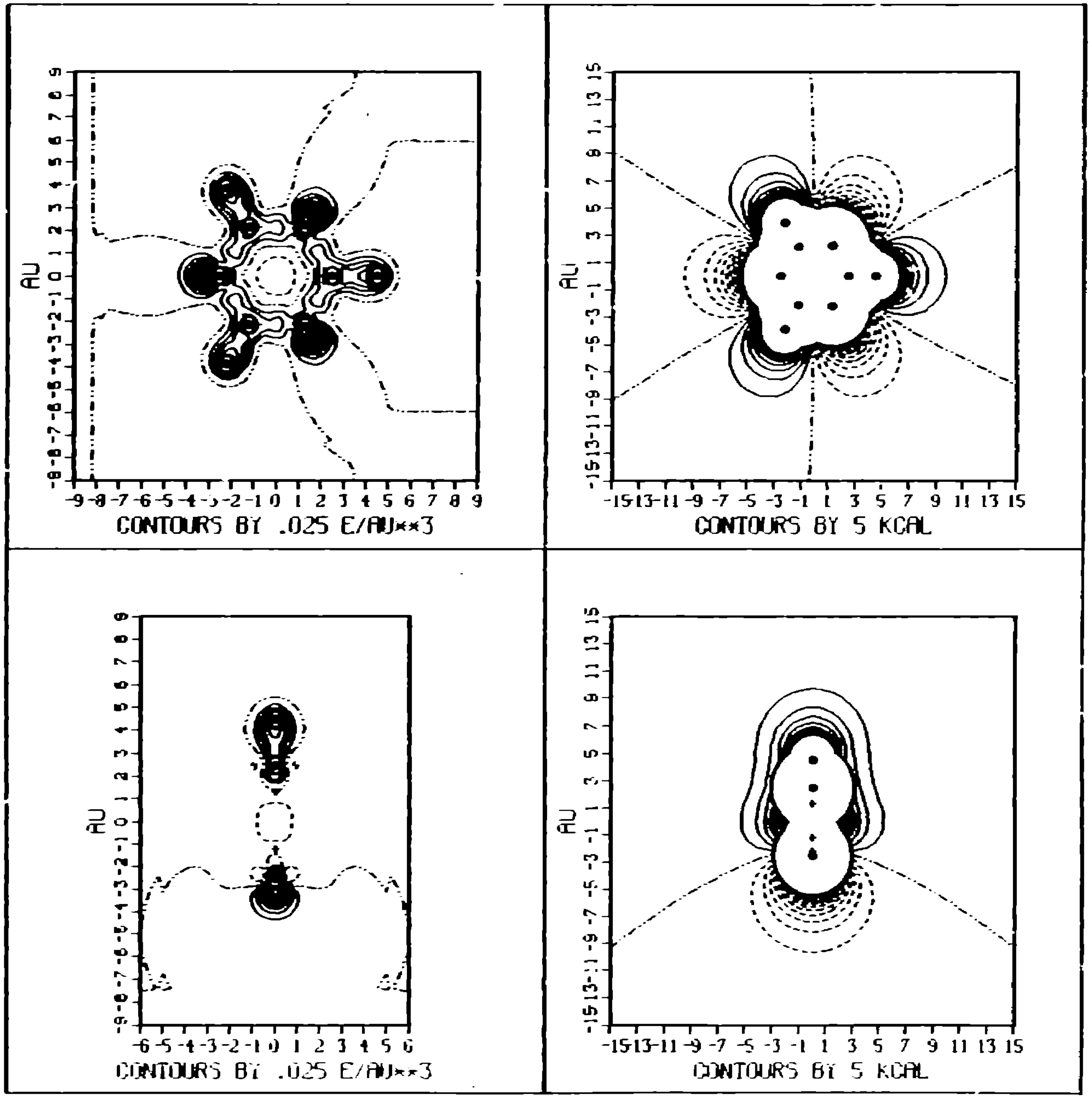
AU
CONTOURS BY .025 E/AU**3
AU
CONTOURS BY 5 KCAL
AU
CONTOURS BY .025 E/AU**3
AU
CONTOURS BY 5 KCAL

Figure 11

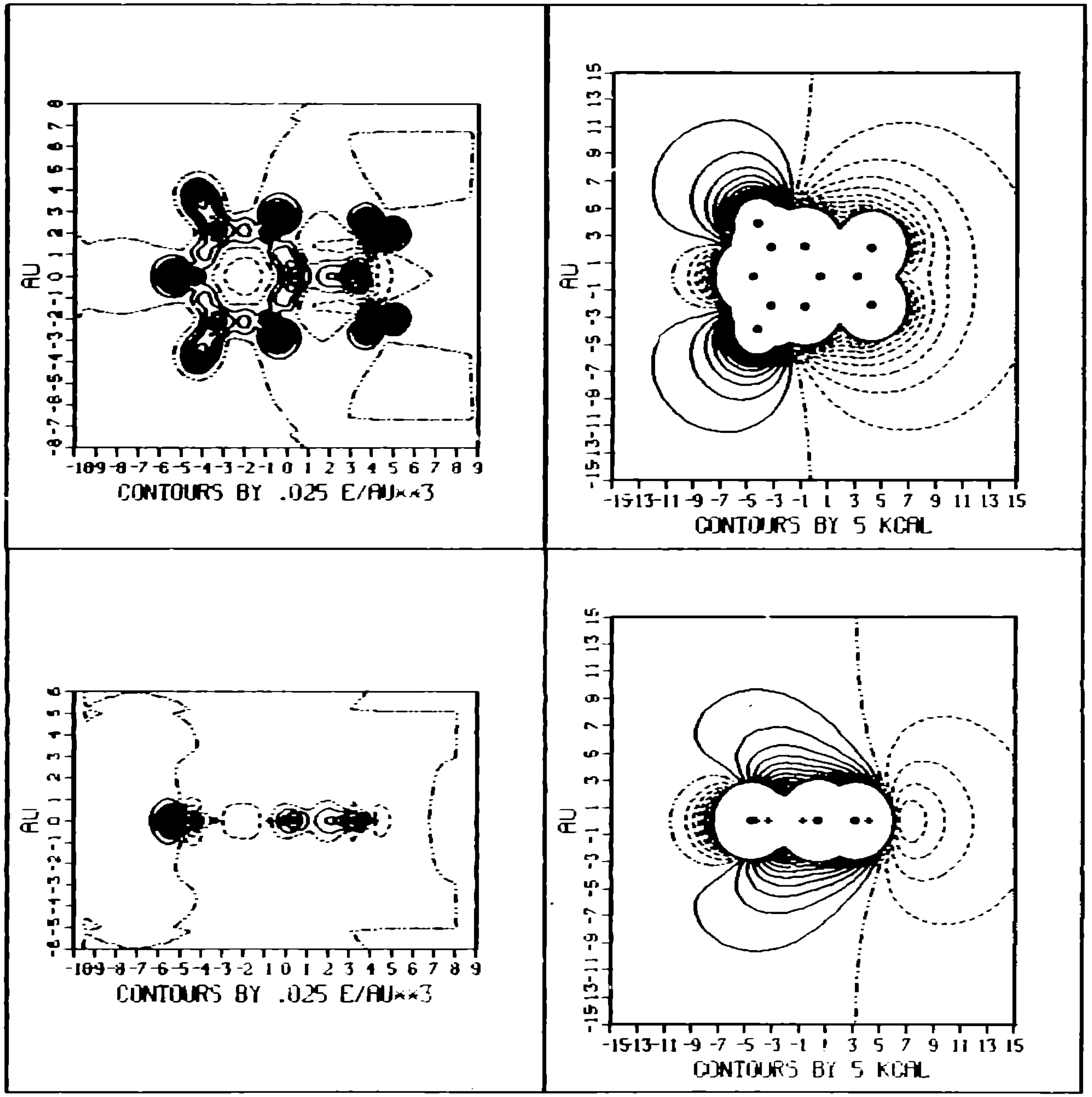
AU
-10 9 -8 -7 -6 -5 -4 -3 -2 -1 0 1 2 3 4 5 6 7 8 9
CONTOURS BY .025 E/AU**3
AU
-15 13 -11 -9 -7 -5 -3 -1 1 3 5 7 9 11 13 15
CONTOURS BY 5 KCAL
AU
-10 9 -8 -7 -6 -5 -4 -3 -2 -1 0 1 2 3 4 5 6 7 8 9
CONTOURS BY .025 E/AU**3
AU
-15 13 -11 -9 -7 -5 -3 -1 1 3 5 7 9 11 13 15
CONTOURS BY 5 KCAL

Figure 12

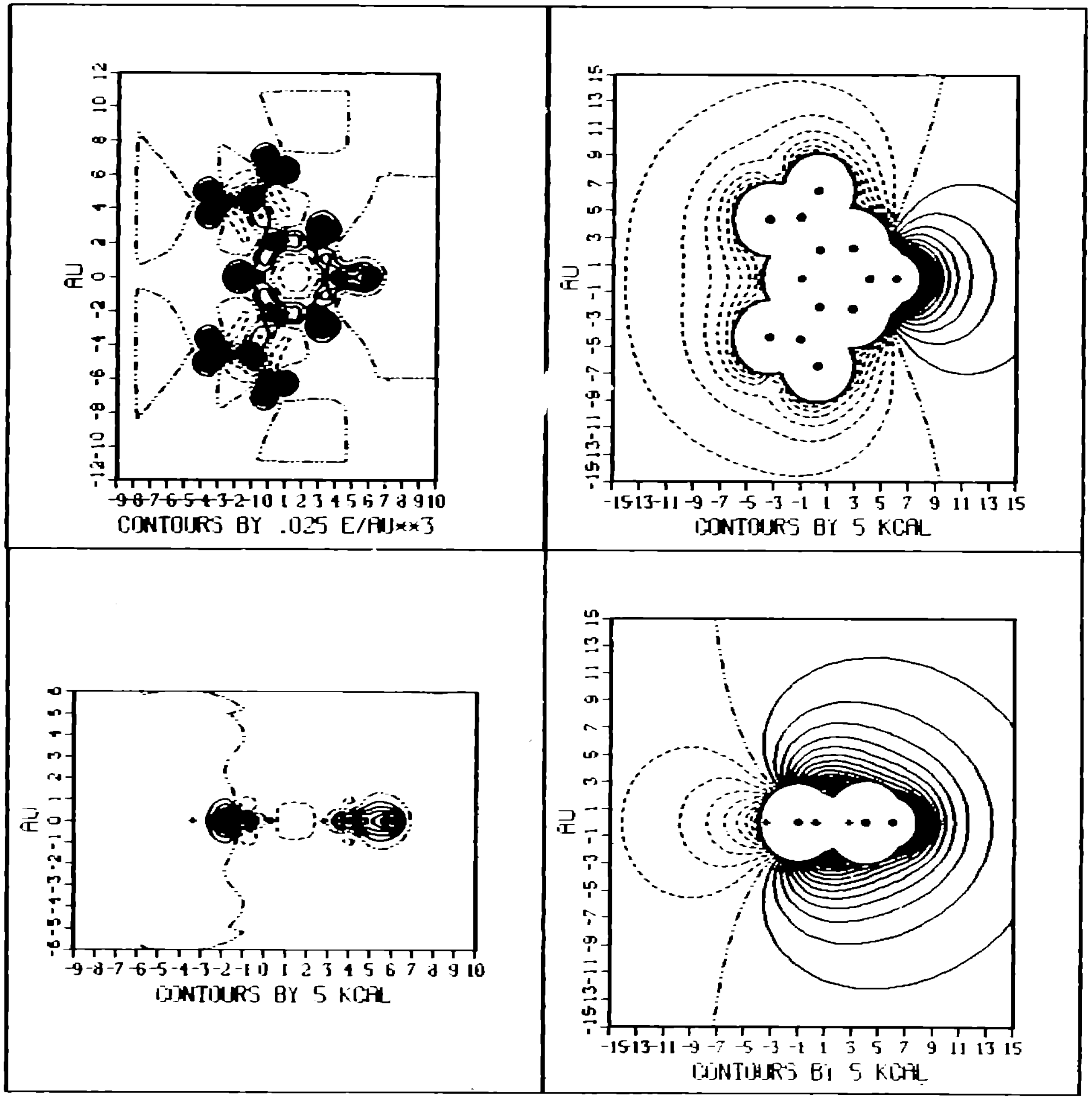
AU
-12 -10 -8 -6 -4 -2 0 2 4 6 8 10 12
-9 -8 -7 -6 -5 -4 -3 -2 -1 0 1 2 3 4 5 6 7 8 9 10
CONTOURS BY .025 E/AU**3
AU
-15 -13 -11 -9 -7 -5 -3 -1 1 3 5 7 9 11 13 15
-15 -13 -11 -9 -7 -5 -3 -1 1 3 5 7 9 11 13 15
CONTOURS BY 5 KCAL
AU
-6 -5 -4 -3 -2 -1 0 1 2 3 4 5 6
-9 -8 -7 -6 -5 -4 -3 -2 -1 0 1 2 3 4 5 6 7 8 9 10
CONTOURS BY 5 KCAL
AU
-15 -13 -11 -9 -7 -5 -3 -1 1 3 5 7 9 11 13 15
-15 -13 -11 -9 -7 -5 -3 -1 1 3 5 7 9 11 13 15
CONTOURS BY 5 KCAL

Figure 13

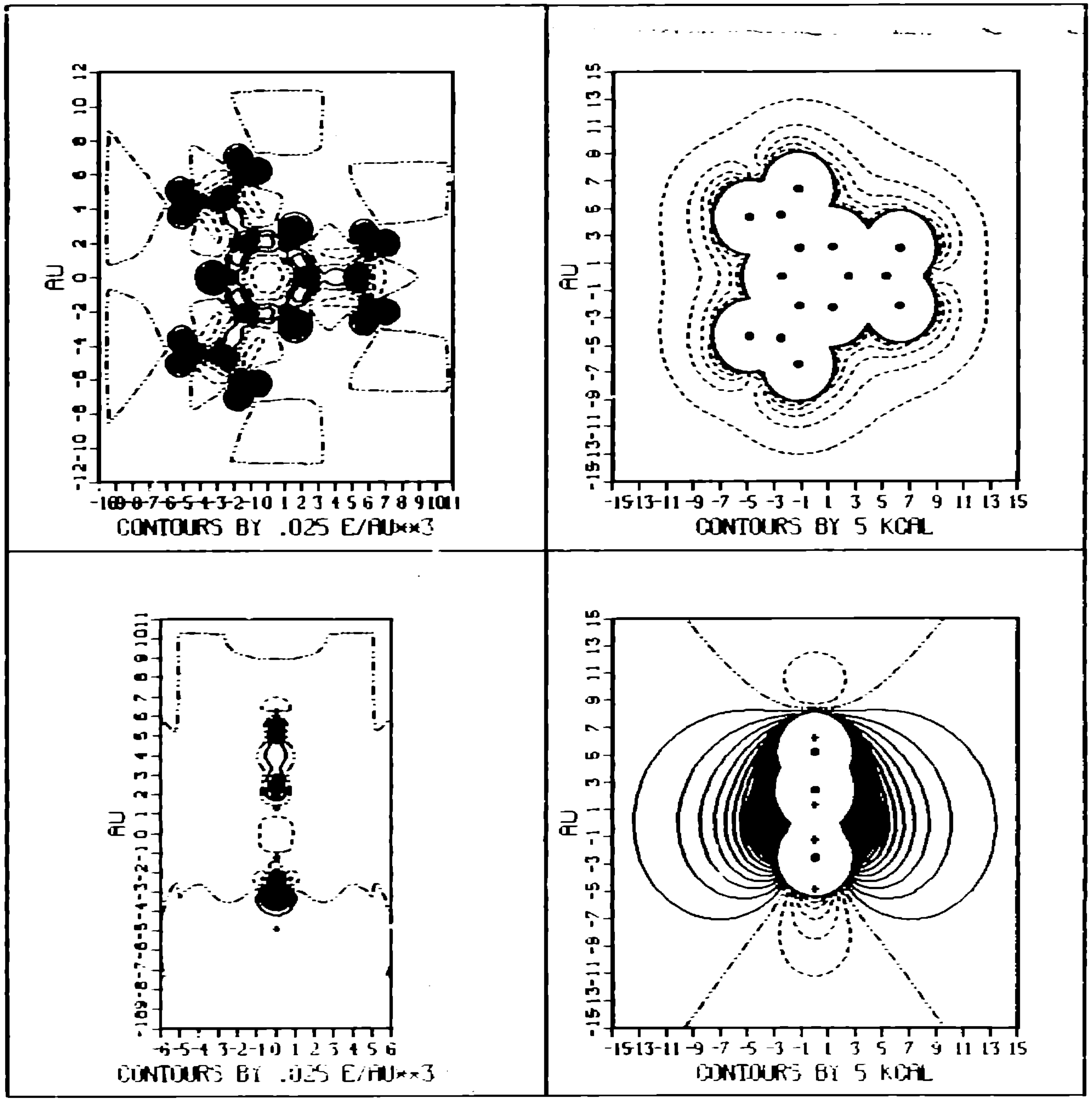
AU
-10-9-8-7-6-5-4-3-2-1 0 1 2 3 4 5 6 7 8 9 10 11
CONTOURS BY .025 E/AU**3
AU
-15-13-11 -9 -7 -5 -3 -1 1 3 5 7 9 11 13 15
CONTOURS BY 5 KCAL
AU
-6-5-4-3-2-1 0 1 2 3 4 5 6
CONTOURS BY .025 E/AU**3
AU
-15-13-11 -9 -7 -5 -3 -1 1 3 5 7 9 11 13 15
CONTOURS BY 5 KCAL

Figure 14

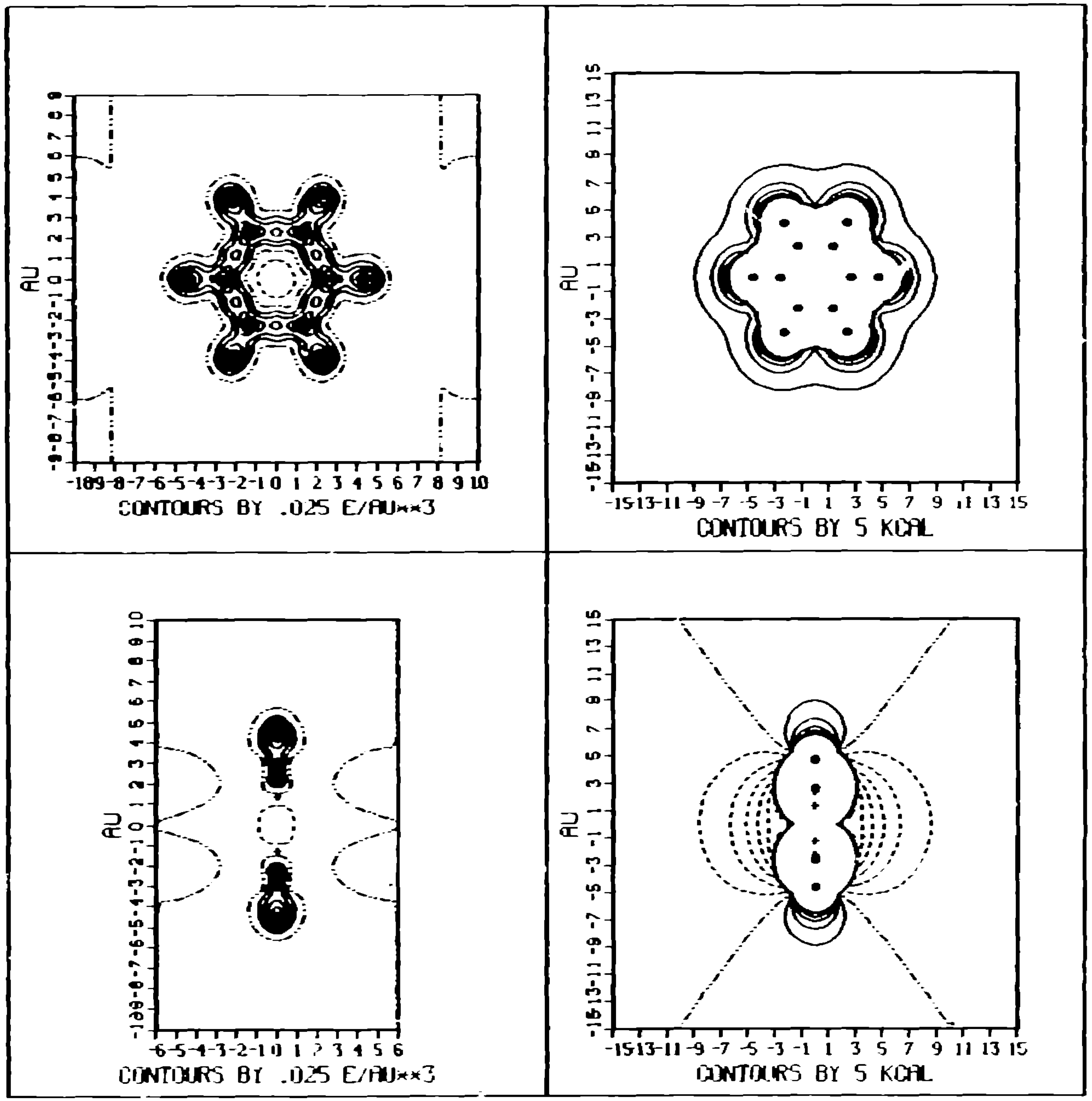
AU
-10 -9 -8 -7 -6 -5 -4 -3 -2 -1 0 1 2 3 4 5 6 7 8 9 10
CONTOURS BY .025 E/AU**3
AU
-15 -13 -11 -9 -7 -5 -3 -1 1 3 5 7 9 11 13 15
CONTOURS BY 5 KCAL
AU
-6 -5 -4 -3 -2 -1 0 1 2 3 4 5 6
CONTOURS BY .025 E/AU**3
AU
-15 -13 -11 -9 -7 -5 -3 -1 1 3 5 7 9 11 13 15
CONTOURS BY 5 KCAL

Figure 15

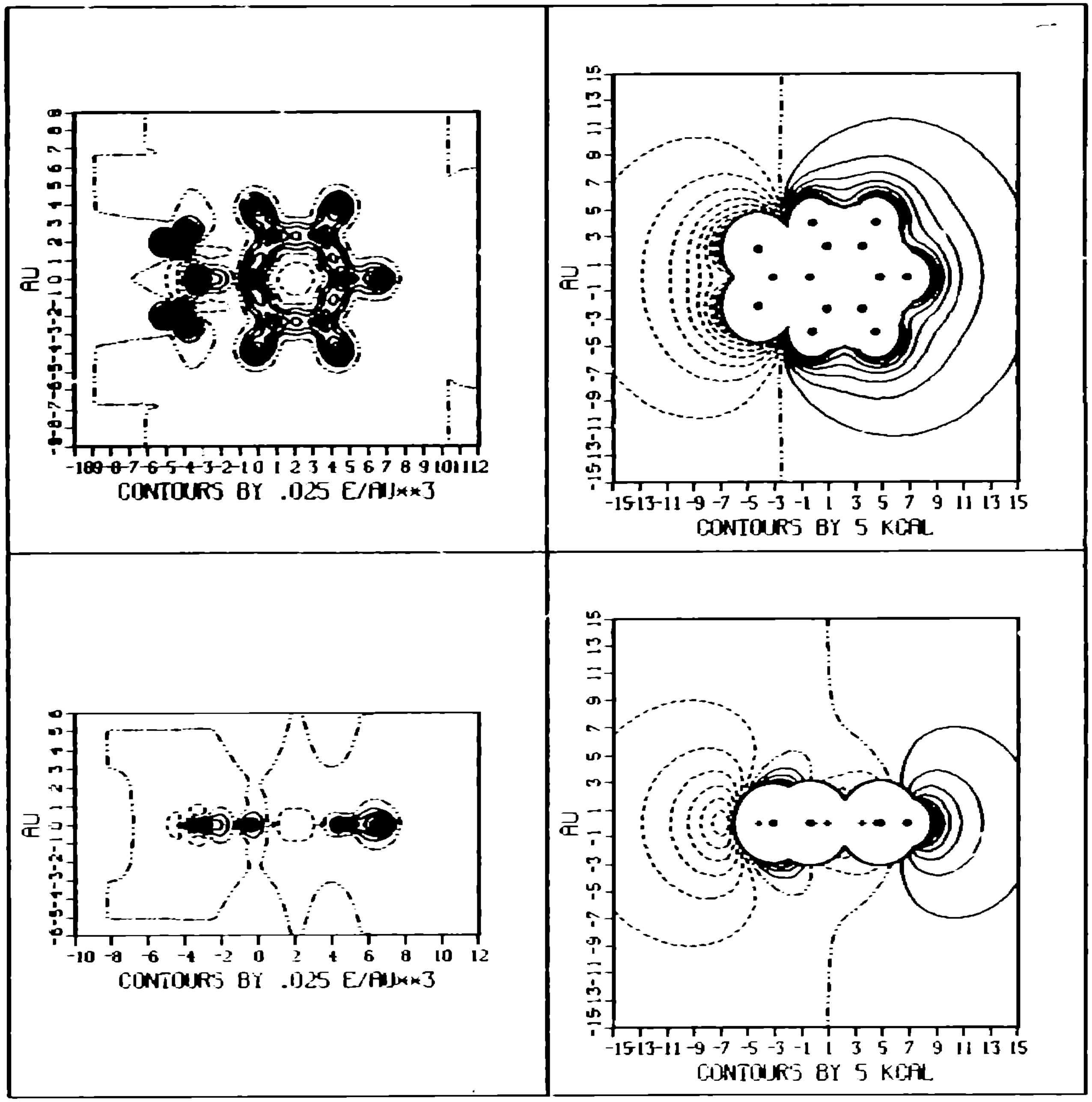
AU
-10 9 8 7 6 5 4 3 2 1 0 1 2 3 4 5 6 7 8 9 10 11 12
CONTOURS BY .025 E/AU**3
AU
-15 13 11 9 7 5 3 1 1 3 5 7 9 11 13 15
-15 13 -11 -9 -7 -5 -3 -1 1 3 5 7 9 11 13 15
CONTOURS BY 5 KCAL
AU
-10 -8 -6 -4 -2 0 2 4 6 8 10 12
CONTOURS BY .025 E/AU**3
AU
-15 13 11 9 7 5 3 1 1 3 5 7 9 11 13 15
-15 13 -11 -9 -7 -5 -3 -1 1 3 5 7 9 11 13 15
CONTOURS BY 5 KCAL

Figure 16

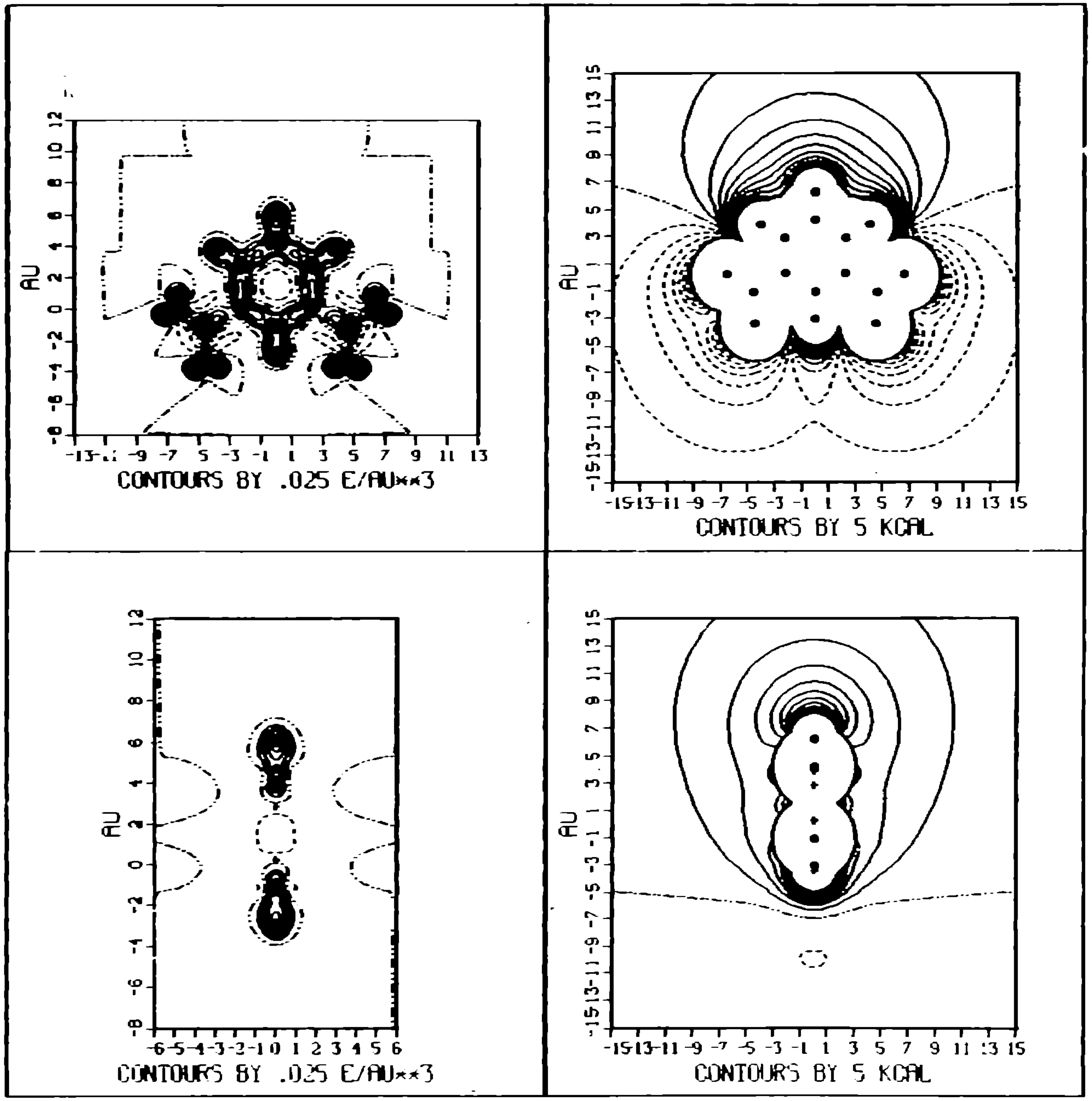
AU
CONTOURS BY .025 E/AU**3
AU
CONTOURS BY 5 KCAL
AU
CONTOURS BY .025 E/AU**3
AU
CONTOURS BY 5 KCAL

Figure 17

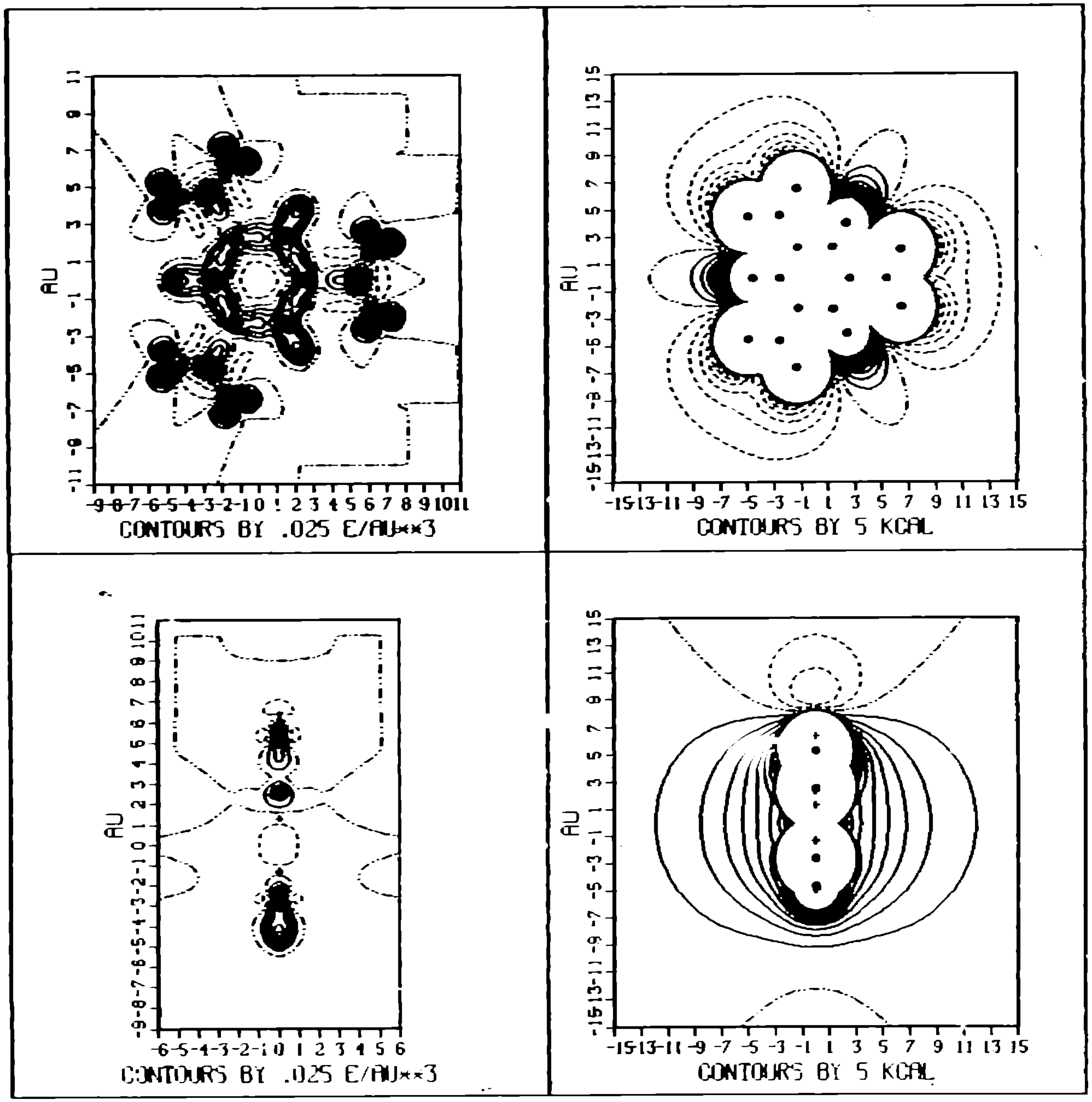
AU
-11 -9 -7 -5 -3 -1 1 3 5 7 9 11
-9 -8 -7 -6 -5 -4 -3 -2 -1 0 1 2 3 4 5 6 7 8 9 10 11
CONTOURS BY .025 E/AU**3
AU
-15 -13 -11 -9 -7 -5 -3 -1 1 3 5 7 9 11 13 15
-15 -13 -11 -9 -7 -5 -3 -1 1 3 5 7 9 11 13 15
CONTOURS BY 5 KCAL
AU
-9 -8 -7 -6 -5 -4 -3 -2 -1 0 1 2 3 4 5 6 7 8 9 10 11
-6 -5 -4 -3 -2 -1 0 1 2 3 4 5 6
CONTOURS BY .025 E/AU**3
AU
-15 -13 -11 -9 -7 -5 -3 -1 1 3 5 7 9 11 13 15
-15 -13 -11 -9 -7 -5 -3 -1 1 3 5 7 9 11 13 15
CONTOURS BY 5 KCAL